Localization of Chaotic Resonance States due to a Partial Transport Barrier

Martin J. Körber,[1] Arnd Bäcker,[1,2] and Roland Ketzmerick[1,2]
[1]*Technische Universität Dresden, Institut für Theoretische Physik and Center for Dynamics, 01062 Dresden, Germany*
[2]*Max-Planck-Institut für Physik komplexer Systeme, Nöthnitzer Straße 38, 01187 Dresden, Germany*
(Received 2 September 2015; published 15 December 2015)

Chaotic eigenstates of quantum systems are known to localize on either side of a classical partial transport barrier if the flux connecting the two sides is quantum mechanically not resolved due to Heisenberg's uncertainty. Surprisingly, in open systems with escape chaotic resonance states can localize even if the flux is quantum mechanically resolved. We explain this using the concept of conditionally invariant measures from classical dynamical systems by introducing a new quantum mechanically relevant class of such fractal measures. We numerically find quantum-to-classical correspondence for localization transitions depending on the openness of the system and on the decay rate of resonance states.

DOI: 10.1103/PhysRevLett.115.254101 PACS numbers: 05.45.Mt, 03.65.Sq, 05.45.Df

Localization of quantum eigenstates and wave packets is of fundamental importance for the physics of transport and appears for a variety of reasons, e.g., strong localization due to disorder [1], weak localization due to time-reversal symmetry [2], localized edge states due to topological protection [3], or localization due to classically restrictive phase-space structures [4]. In the latter case, the localization can originate from impenetrable barriers of regular motion or partial transport barriers with a small transmission given by a flux Φ within a chaotic region [4–11]. Such partial barriers are ubiquitous in the chaotic region of generic two degree-of-freedom Hamiltonian systems [5,6,9] and a universal localization transition was found [12]. Chaotic eigenstates of the system typically localize on either side of a partial barrier if the transmission region is quantum mechanically not resolved, i.e., if the classical flux Φ across the partial barrier is much smaller than the size h of Planck's cell ($\Phi \ll h$). If the transmission region is quantum mechanically resolved ($h \ll \Phi$), eigenstates are equipartitioned in the chaotic component, thereby ignoring the presence of the partial barrier.

In contrast, in open Hamiltonian systems which allow for escape [13–23], chaotic resonance states exhibit localization in the presence of a partial barrier surprisingly even in the semiclassical regime ($h \ll \Phi$) [24]. Such a localized state is shown in Fig. 1, upper right, by its Husimi phase-space representation. This demonstrates that in open systems the influence of partial barriers on localization and transport properties is even more substantial than in closed systems. A thorough understanding of this localization phenomenon remains open, so far. A prominent application are optical microcavities, where the emission patterns are governed by the localization of eigenmodes [25–33]. For their design, it is particularly important to know whether a partial barrier is desired to enhance localization or whether it should be avoided. The localization phenomenon may also have relevance in many other areas of physics, such as transport through quantum dots [34], ionization of driven Rydberg atoms [35], and microwave cavities [36].

Since the localization appears in a semiclassical regime ($h \ll \Phi$), one may wonder if it has a classical origin. Thus, one needs the classical counterpart of a quantum resonance state. This is given in the field of open dynamical systems [13,37–44] by a conditionally invariant measure (CIM). It is invariant under time evolution up to an exponential decay

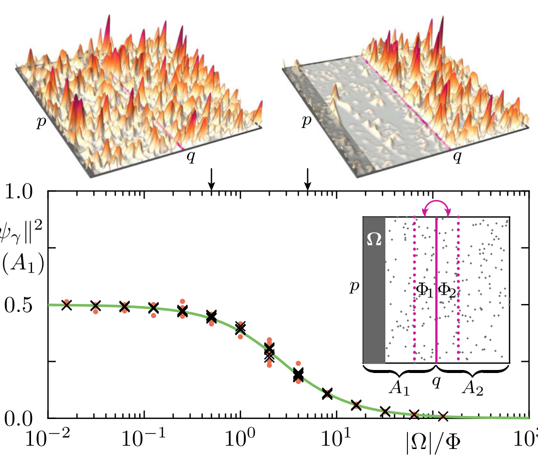

FIG. 1 (color online). Weight $\|P_1\psi_\gamma\|^2$ (symbols) of resonance states in region A_1 vs ratio of size $|\Omega|$ of opening and flux Φ across a partial barrier for different parameters of the partial-barrier standard map ($16 \leq \Phi/h, |\Omega|/h \leq 2048$; $|A_1| = 0.5$; $h = 1/6000$). Weight of state with γ closest to $\gamma_{\rm nat}$ (red points) and averaged over states with decay rates $\gamma \in [\gamma_{\rm nat}/1.1, 1.1\,\gamma_{\rm nat}]$ (black crosses). This is compared to the natural CIM $\mu_{\rm nat}(A_1)$ [Eq. (4), solid green line]. Inset: Phase space of the partial-barrier map, illustrating regions A_1, A_2 on either side of the partial barrier (solid magenta line) with exchanging regions Φ_1, Φ_2, and opening Ω. Upper panels: Husimi representation of typical resonance states with $\gamma \approx \gamma_{\rm nat}$ for $h = 1/1000$, $\Phi/h = 20$, and two values $|\Omega|/\Phi$ indicated by arrows.

 © 2015 American Physical Society

with rate γ. The asymptotic decay of generic initial phase-space distributions leads to the so-called natural CIM $\mu_{\rm nat}$ with decay rate $\gamma_{\rm nat}$. The quantum-mechanical relevance of $\mu_{\rm nat}$ is shown in [13–15,27,41]. Note that the steady probability distribution introduced in the context of optical microcavities [27] corresponds to $\mu_{\rm nat}$. The natural CIM $\mu_{\rm nat}$ for the single decay rate $\gamma_{\rm nat}$, however, cannot be the classical counterpart for all quantum resonance states as they have a wide range of decay rates (see, e.g., Fig. 2). Exceptional CIMs with decay rate γ different from $\gamma_{\rm nat}$ have been discussed [40,41]. In fact, for each γ one can construct infinitely many CIMs. It is an open question which of these CIMs correspond to quantum resonance states for arbitrary γ. To answer this question one has to go beyond the important results of Ref. [18] which relate the total weight of a resonance state on each forward escaping set to its decay rate.

In this Letter, we introduce the quantum mechanically relevant class of CIMs. Their localization explains the localization of chaotic resonance states in the presence of a partial barrier. In particular, we find (i) a transition from equipartition to localization when opening the system, Fig. 1, and (ii) a transition from localization on one side of the partial barrier to localization on the other side for resonance states with increasing decay rate, Fig. 2. We numerically demonstrate quantum-to-classical correspondence for a designed partial-barrier map and the generic standard map.

Partial-barrier map.—We design a chaotic model map with a single partial barrier (similar to Ref. [24]), which allows for numerically varying the flux across the partial barrier and for deriving the classical localization, Eq. (4).

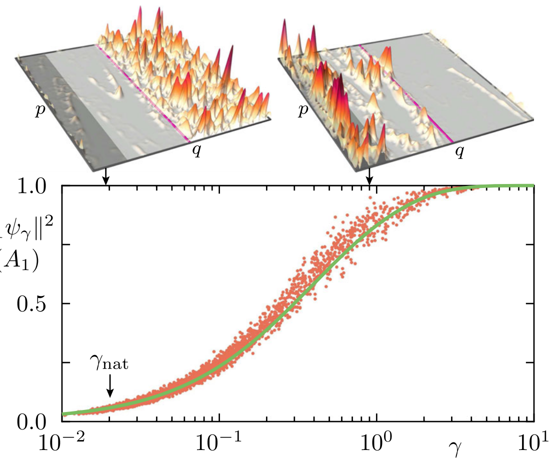

FIG. 2 (color online). Weight $\|P_1\psi_\gamma\|^2$ (red points) of resonance states ψ_γ in region A_1 vs decay rate γ for the partial-barrier standard map ($\Phi/h = 64$; $|\Omega|/h = 1024$; $|A_1| = 0.5$; $h = 1/6000$). This is compared to the γ-natural CIM $\mu_\gamma(A_1)$ [Eq. (4), solid green line]. Upper panels: Husimi representation of typical long-lived (left) and short-lived (right) resonance state for $h = 1/1000$ with γ values indicated by arrows.

The partial-barrier map $T = M \circ E \circ O$ is a composition of three maps: the map M describes the unconnected chaotic dynamics within two regions, A_k. They decompose the phase space $\Gamma = [0,1) \times [0,1)$ into $A_1 = [0,|A_1|) \times [0,1)$ and its complement $A_2 = \Gamma \backslash A_1$; see the inset in Fig. 1, where $|A_1|$ denotes the area of A_1 and by normalization, $|A_2| = 1 - |A_1|$. The map E induces a flux Φ between A_1 and A_2 by exchanging regions $\Phi_k \subset A_k$ with $|\Phi_k| = \Phi$. The map O opens the system by the absorbing region Ω, which is contained in region A_1.

We introduce two different dynamics for M. For the numerical analysis, we use the generic standard map [45] on the torus in symmetrized form, $q_{t+1} = q_t + p_t^*$, $p_{t+1} = p_t^* + v(q_{t+1})$ with $p_t^* = p_t + v(q_t)$ for $v(q) = (\kappa/4\pi)\sin(2\pi q)$ acting individually on each of the regions A_k after appropriate rescaling. We fix $\kappa = 10$ where the standard map displays a fully chaotic phase space. For analytical considerations, we use the ternary Baker map in each region A_k, as illustrated in Fig. 3(a), which allows for the derivation of Eq. (4). We refer to the corresponding maps T as partial-barrier standard map and partial-barrier Baker map, respectively.

Quantum localization transitions.—Let us consider the quantization U of the partial-barrier standard map T. From the eigenvalue problem for U,

$$U\psi_\gamma = e^{-\gamma/2} e^{i\theta} \psi_\gamma, \tag{1}$$

we numerically compute the decay rates γ, describing the temporal decay of the norm, $\|U^t\psi_\gamma\|^2 = e^{-\gamma t}$, and the corresponding resonance states ψ_γ (the phase θ is not relevant in the following). The absolute weight of ψ_γ in region A_1 is given by $\|P_1\psi_\gamma\|^2$, where P_1 denotes the projection onto the subspace associated to A_1. We observe (i) a transition from equipartition to localization on A_2 for increasing size $|\Omega|$ of the opening, see Fig. 1, and (ii) a transition from localization on A_2 to localization on A_1 for increasing γ, see Fig. 2. Transition (i) is surprising as localization occurs for $h \ll \Phi$, where in the closed system all eigenstates are equipartitioned [12]. Transition (ii) shows that in open systems the localization depends on the decay rate γ.

In Fig. 1, we focus on resonances with decay rate $\gamma \approx \gamma_{\rm nat}$, which describes the decay of typical long-lived resonance states in the semiclassical limit. We find transition (i) from equipartition, $\|P_1\psi_\gamma\|^2 = |A_1|$, for $|\Omega| \ll \Phi$ to localization on A_2 for $|\Omega| \gg \Phi$ for various values of Φ/h and $|\Omega|/h$. The transition is universal with the scaling parameter $|\Omega|/\Phi$. Moreover, this even holds for individual states without averaging (red dots). We stress that this localization transition in the open system occurs even though $\Phi/h \geq 10$, where in the closed system all eigenstates are equipartitioned [12].

In Fig. 2, we fix the parameters such that $|\Omega| \gg \Phi$, for which the long-lived resonance states localize on A_2, and show the γ dependence of the weights $\|P_1\psi_\gamma\|^2$ for all resonance states. We find transition (ii) from resonance states which localize on A_2 for small γ to resonance states which localize on A_1 for large γ, including equipartitioned resonance states in between.

The fact that both transitions (i) and (ii) occur for $h \ll \Phi$ suggests that the localization transitions could be of classical origin. Furthermore, from the point of view of decaying classical distributions, the observed transitions qualitatively seem to be rather intuitive: in Fig. 1, for a larger size of the opening one has less weight in region A_1. In Fig. 2, a larger weight in A_1 corresponds to a larger decay rate. For a quantitative description, however, one needs to find the quantum mechanically relevant class of CIMs.

Classical localization.—A CIM μ_γ is defined by

$$\mu_\gamma[T^{-1}(X)] = e^{-\gamma}\mu_\gamma(X), \tag{2}$$

for each measurable subset X of phase space. It is invariant under the classical iterative dynamics T of the open system up to an exponential decay with rate γ. Equation (2) states that the measure $\mu_\gamma[T^{-1}(X)]$ of the set $T^{-1}(X)$ that will be mapped to X is smaller than $\mu_\gamma(X)$ by the factor $e^{-\gamma}$. These measures must be zero on the iterates of the opening Ω. Thus, the support of μ_γ is the fractal backward trapped set Γ_b [horizontal black stripes in Fig. 3(b)], that is the set of points in phase space which do not escape under backward

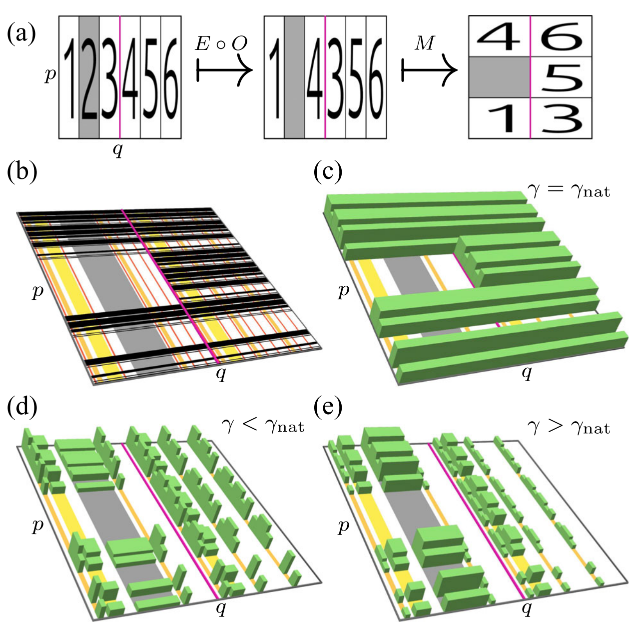

FIG. 3 (color online). (a) Illustration of the partial-barrier Baker map $T = M\circ E\circ O$. Magenta line indicates partial barrier and gray shaded region marks the opening (left and central) and image of opening (right). (b) Backward trapped set (dark horizontal stripes) and forward escaping sets Ω (gray), $T^{-1}(\Omega)$ (yellow), $T^{-2}(\Omega)$ (orange), and $T^{-3}(\Omega)$ (red). (c) Natural CIM integrated over boxes of size 3^{-3} in the p direction. (d),(e) Approximation of γ-natural CIMs by truncation of Eq. (3) to $n \leq 2$ for $\gamma \neq \gamma_{\rm nat}$.

time evolution. Particularly important is the natural CIM $\mu_{\rm nat}$, see Fig. 3(c), which is constant on its support [because of integration over boxes in Fig. 3(c) one finds two nonzero box measures].

We now generalize $\mu_{\rm nat}$ to a CIM μ_γ of arbitrary decay rate γ, which we call γ-natural CIM. To this end, we use a construction of CIMs [40,41] where one starts with an arbitrary probability measure on the intersection $\Omega\cap\Gamma_b$ of the opening Ω with the backward trapped set Γ_b. By propagating this measure backwards to all forward escaping sets $T^{-n}(\Omega)$ [vertical colored stripes in Fig. 3(b)] and appropriate scaling [respecting the decay rate γ, Eq. (2)] one obtains a CIM. Here, we choose the simplest measure on $\Omega\cap\Gamma_b$, given by $\mu_{\rm nat}$. This choice of a measure, which is constant on its support, is quantum mechanically motivated in analogy to quantum ergodicity for closed fully chaotic systems, where eigenstates in the semiclassical limit approach the constant invariant measure [46,47]. This choice leads to the γ-natural CIM

$$\mu_\gamma(X) = \mathcal{N}\sum_{n=0}^{\infty} e^{(\gamma_{\rm nat}-\gamma)n}\mu_{\rm nat}[X\cap T^{-n}(\Omega)], \tag{3}$$

with normalization $\mathcal{N} = (1-e^{-\gamma})/(1-e^{-\gamma_{\rm nat}})$. This series multiplies $\mu_{\rm nat}$ in each forward escaping set $T^{-n}(\Omega)$ by an appropriate factor which imposes the overall decay rate γ according to Eq. (2). Two examples of γ-natural CIMs for the partial-barrier Baker map are shown in Figs. 3(d) and 3(e). The measure is constant on $T^{-n}(\Omega)\cap\Gamma_b$ for each $n \in \mathbb{N}_0$. With increasing n, this constant is decreasing (increasing) for $\gamma > \gamma_{\rm nat}$ ($\gamma < \gamma_{\rm nat}$); in particular, short-lived measures μ_γ have more weight in the opening. Note that the idea underlying Eq. (3) was used without the notion of CIMs in Ref. [18] for sets $X = T^{-n}(\Omega)$ for systems without a partial barrier. Moreover, note that the γ-natural CIMs are solutions of the exact Perron-Frobenius operator (which is not available), but cannot be obtained from finite-dimensional approximations. Therefore, they have to be constructed directly in phase space.

We find as our main result on the classical localization of μ_γ due to a partial barrier that the weight of μ_γ on each side of the partial barrier is given by [48]

$$\mu_\gamma(A_1) = \frac{\mu_{\rm nat}(A_1) - c_\gamma}{1 - c_\gamma}, \tag{4}$$

and $\mu_\gamma(A_2) = 1 - \mu_\gamma(A_1)$, with

$$c_\gamma = (1 - e^{\gamma-\gamma_{\rm nat}})(1 - e^{-\gamma_{\rm nat}})\frac{|A_1|}{|\Omega|}\frac{|A_2|}{\Phi}. \tag{5}$$

The values for $\mu_{\rm nat}(A_1)$ and $\gamma_{\rm nat}$ follow from the longest-lived eigenstate of the eigenvalue problem

$$F_{\rm nat}\begin{pmatrix}\mu_{\rm nat}(A_1)\\ \mu_{\rm nat}(A_2)\end{pmatrix} = e^{-\gamma_{\rm nat}}\begin{pmatrix}\mu_{\rm nat}(A_1)\\ \mu_{\rm nat}(A_2)\end{pmatrix}, \tag{6}$$

where F_{nat} denotes the transition matrix between A_1 and A_2 for the one-step propagation of μ_{nat} (see Ref. [49] for approximations of the Perron-Frobenius operator). In general, F_{nat} may be obtained numerically or it may be approximated by assuming a uniform distribution for μ_{nat},

$$F_{\mathrm{nat}} \approx \begin{pmatrix} 1 - (|\Omega| + \Phi)/|A_1| & \Phi/|A_2| \\ \Phi/|A_1| & 1 - \Phi/|A_2| \end{pmatrix}. \quad (7)$$

This turns out to be quite a good approximation even for fractal μ_{nat} and it is exact for the partial-barrier Baker map.

Quantum-to-classical correspondence.—Figure 1 (green line) shows the classical localization $\mu_\gamma(A_1)$, Eq. (4), for $\gamma = \gamma_{\mathrm{nat}}$ (i.e., $c_\gamma = 0$ and $\mu_\gamma = \mu_{\mathrm{nat}}$), using the approximation Eq. (7). When increasing the size $|\Omega|$ of the opening, we find a transition from equipartition for $|\Omega| \ll \Phi$ to localization for $|\Omega| \gg \Phi$. The only scaling parameters are $|\Omega|/\Phi$ and $|A_1|/|A_2|$. We find very good agreement of the classical localization measure with the localization of the quantum resonance states. Note that for $\gamma \neq \gamma_{\mathrm{nat}}$, the localization depends on all parameters $|\Omega|$, Φ, and $|A_1|$.

Figure 2 (green line) shows Eq. (4) as a function of γ. The classical localization measure $\mu_\gamma(A_1)$ monotonically increases with γ; i.e., the faster the decay, the larger is the weight in region A_1 with the opening Ω. In the limit $\gamma \to \infty$ one finds $\mu_\gamma(A_1) = 1$, and in fact, all the weight is in the opening Ω. In the limit $\gamma \to 0$ one finds a small constant $\mu_0(A_1) > 0$; i.e., even though most of the weight is in A_2 there is always a small contribution in A_1 due to the exchange between A_1 and A_2. Again, we find very good agreement between the classical localization measure and the localization of the quantum resonance states for all decay rates γ. Note that quantum-to-classical correspondence is also confirmed for $|A_1| \neq |A_2|$ (not shown).

Do these results for the partial-barrier map generalize to generic systems? In Fig. 4, we show for the standard map at $\kappa = 2.9$, where it has a mixed phase space, that the localization of the chaotic resonance states on region A_1, which contains the opening, increases as a function of γ. Qualitatively, we find the same localization behavior as for the partial-barrier standard map in Fig. 2. Quantitatively, it is well described by the classical localization of μ_γ, which is determined numerically [48]. Also the analytical prediction, Eq. (4), works reasonably well. Overall, Figs. 1, 2, and 4 demonstrate quantum-to-classical correspondence for the localization of chaotic resonance states in open systems due to a partial barrier.

Outlook.—We see the following future challenges: (a) While in this work we concentrate on the weights on either side of a partial barrier, one should verify the quantum-to-classical correspondence for the fine-structure of chaotic resonance states to γ-natural CIMs. (b) Which deviations arise when approaching the quantum regime of $h \approx \Phi$, $|\Omega|$? (c) Is the new class of γ-natural CIMs, which is quantum mechanically motivated, of relevance also in classical dynamical systems? (d) Is it possible to predict which quantum mechanical decay rates γ occur in the presence of a partial barrier including their distribution, as it is known for fully chaotic systems [20,50,51]? (e) The present work explains the localization of resonance states which have been used to derive the hierarchical fractal Weyl laws [24] for a hierarchy of partial barriers. Now it is possible to discuss whether these laws survive in the semiclassical limit. (f) We see direct applications to mode coupling in optical microcavities [52] and in recently studied parity-time symmetric systems [53,54], where instead of a partial barrier one has coupled symmetry-related subspaces.

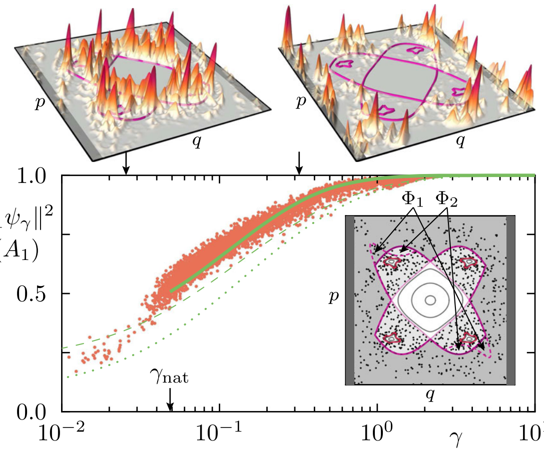

FIG. 4 (color online). Weight $\|P_1\psi_\gamma\|^2$ (red points) of resonance states ψ_γ in region A_1 vs decay rate γ for standard map at $\kappa = 2.9$, with $|A_1| \approx 0.6664$, $|A_2| \approx 0.2061$, $\Phi \approx 0.0126$, $|\Omega| = 0.1$, and $h = 1/10000$. This is compared to the γ-natural CIM $\mu_\gamma(A_1)$, either by direct numerical computation [48] (solid green line), using Eq. (4) and computing F_{nat} numerically (dashed green line), or by using approximation Eq. (7) (dotted green line). Inset: Phase space of the standard map with regular and chaotic regions, illustrating regions A_1 (medium gray shaded), A_2 (light gray shaded) on either side of the main partial barrier (thick solid magenta line) with exchanging regions Φ_1, Φ_2, and opening Ω (dark gray shaded). Upper panels: Husimi representation of typical long-lived (left) and short-lived (right) resonance states for $h = 1/1000$ with γ values indicated by arrows.

We are grateful to E. G. Altmann, K. Clauß, S. Nonnenmacher, and H. Schomerus for helpful comments and stimulating discussions, and acknowledge financial support through the Deutsche Forschungsgemeinschaft under Grant No. KE 537/5-1.

[1] P. W. Anderson, Absence of diffusion in certain random lattices, Phys. Rev. **109**, 1492 (1958).

[2] G. Bergmann, Weak localization in thin films, Phys. Rep. **107**, 1 (1984).

[3] X.-L. Qi and S.-C. Zhang, Topological insulators and superconductors, Rev. Mod. Phys. **83**, 1057 (2011).

[4] O. Bohigas, S. Tomsovic, and D. Ullmo, Manifestations of classical phase space structures in quantum mechanics, Phys. Rep. **223**, 43 (1993).
[5] R. S. MacKay, J. D. Meiss, and I. C. Percival, Stochasticity and Transport in Hamiltonian Systems, Phys. Rev. Lett. **52**, 697 (1984).
[6] R. S. MacKay, J. D. Meiss, and I. C. Percival, Transport in Hamiltonian systems, Physica (Amsterdam) **13D**, 55 (1984).
[7] R. C. Brown and R. E. Wyatt, Quantum Mechanical Manifestation of Cantori: Wave-Packet Localization in Stochastic Regions, Phys. Rev. Lett. **57**, 1 (1986).
[8] T. Geisel, G. Radons, and J. Rubner, Kolmogorov-Arnol'd-Moser Barriers in the Quantum Dynamics of Chaotic Systems, Phys. Rev. Lett. **57**, 2883 (1986); **58**, 2506(E) (1987).
[9] J. Meiss, Symplectic maps, variational principles, and transport, Rev. Mod. Phys. **64**, 795 (1992).
[10] R. Ketzmerick, L. Hufnagel, F. Steinbach, and M. Weiss, New Class of Eigenstates in Generic Hamiltonian Systems, Phys. Rev. Lett. **85**, 1214 (2000).
[11] N. T. Maitra and E. J. Heller, Quantum transport through cantori, Phys. Rev. E **61**, 3620 (2000).
[12] M. Michler, A. Bäcker, R. Ketzmerick, H.-J. Stöckmann, and S. Tomsovic, Universal Quantum Localizing Transition of a Partial Barrier in a Chaotic Sea, Phys. Rev. Lett. **109**, 234101 (2012).
[13] E. G. Altmann, J. S. E. Portela, and T. Tél, Leaking chaotic systems, Rev. Mod. Phys. **85**, 869 (2013).
[14] M. Novaes, Resonances in open quantum maps, J. Phys. A **46**, 143001 (2013).
[15] G. Casati, G. Maspero, and D. L. Shepelyansky, Quantum fractal eigenstates, Physica (Amsterdam) **131D**, 311 (1999).
[16] W. T. Lu, S. Sridhar, and M. Zworski, Fractal Weyl Laws for Chaotic Open Systems, Phys. Rev. Lett. **91**, 154101 (2003).
[17] H. Schomerus and J. Tworzydło, Quantum-to-Classical Crossover of Quasibound States in Open Quantum Systems, Phys. Rev. Lett. **93**, 154102 (2004).
[18] J. P. Keating, M. Novaes, S. D. Prado, and M. Sieber, Semiclassical Structure of Chaotic Resonance Eigenfunctions, Phys. Rev. Lett. **97**, 150406 (2006).
[19] S. Nonnenmacher and E. Schenck, Resonance distribution in open quantum chaotic systems, Phys. Rev. E **78**, 045202 (2008).
[20] S. Nonnenmacher and M. Zworski, Quantum decay rates in chaotic scattering, Acta Math. **203**, 149 (2009).
[21] L. Ermann, G. G. Carlo, and M. Saraceno, Localization of Resonance Eigenfunctions on Quantum Repellers, Phys. Rev. Lett. **103**, 054102 (2009).
[22] T. Weich, S. Barkhofen, U. Kuhl, C. Poli, and H. Schomerus, Formation and interaction of resonance chains in the open three-disk system, New J. Phys. **16**, 033029 (2014).
[23] M. Schönwetter and E. G. Altmann, Quantum signatures of classical multifractal measures, Phys. Rev. E **91**, 012919 (2015).
[24] M. J. Körber, M. Michler, A. Bäcker, and R. Ketzmerick, Hierarchical Fractal Weyl Laws for Chaotic Resonance States in Open Mixed Systems, Phys. Rev. Lett. **111**, 114102 (2013).
[25] J. U. Nöckel and A. D. Stone, Ray and wave chaos in asymmetric resonant optical cavities, Nature (London) **385**, 45 (1997).
[26] C. Gmachl, F. Capasso, E. E. Narimanov, J. U. Nöckel, A. D. Stone, J. Faist, D. L. Sivco, and A. Y. Cho, High-power directional emission from microlasers with chaotic resonators, Science **280**, 1556 (1998).
[27] S.-Y. Lee, S. Rim, J.-W. Ryu, T.-Y. Kwon, M. Choi, and C.-M. Kim, Quasiscarred Resonances in a Spiral-Shaped Microcavity, Phys. Rev. Lett. **93**, 164102 (2004).
[28] J. Wiersig and J. Main, Fractal Weyl law for chaotic microcavities: Fresnel's laws imply multifractal scattering, Phys. Rev. E **77**, 036205 (2008).
[29] J. Wiersig and M. Hentschel, Combining Directional Light Output and Ultralow Loss in Deformed Microdisks, Phys. Rev. Lett. **100**, 033901 (2008).
[30] J.-B. Shim, S.-B. Lee, S. W. Kim, S.-Y. Lee, J. Yang, S. Moon, J.-H. Lee, and K. An, Uncertainty-Limited Turnstile Transport in Deformed Microcavities, Phys. Rev. Lett. **100**, 174102 (2008).
[31] S. Shinohara, T. Harayama, T. Fukushima, M. Hentschel, T. Sasaki, and E. E. Narimanov, Chaos-Assisted Directional Light Emission from Microcavity Lasers, Phys. Rev. Lett. **104**, 163902 (2010).
[32] J.-B. Shim, J. Wiersig, and H. Cao, Whispering gallery modes formed by partial barriers in ultrasmall deformed microdisks, Phys. Rev. E **84**, 035202 (2011).
[33] H. Cao and J. Wiersig, Dielectric microcavities: Model systems for wave chaos and non-Hermitian physics, Rev. Mod. Phys. **87**, 61 (2015).
[34] T. Ihn, *Semiconductor Nanostructures: Quantum States and Electronic Transport* (Oxford University Press, New York, 2009).
[35] A. Buchleitner, D. Delande, and J. Zakrzewski, Non-dispersive wave packets in periodically driven quantum systems, Phys. Rep. **368**, 409 (2002).
[36] H.-J. Stöckmann, *Quantum Chaos: An Introduction* (Cambridge University Press, Cambridge, 2007).
[37] G. Pianigiani and J. A. Yorke, Expanding maps on sets which are almost invariant: Decay and chaos, Trans. Am. Math. Soc. **252**, 351 (1979).
[38] H. Kantz and P. Grassberger, Repellers, semi-attractors, and long-lived chaotic transients, Physica (Amsterdam) **17D**, 75 (1985).
[39] T. Tél, Escape rate from strange sets as an eigenvalue, Phys. Rev. A **36**, 1502 (1987).
[40] M. F. Demers and L.-S. Young, Escape rates and conditionally invariant measures, Nonlinearity **19**, 377 (2006).
[41] S. Nonnenmacher and M. Rubin, Resonant eigenstates for a quantized chaotic system, Nonlinearity **20**, 1387 (2007).
[42] Y.-C. Lai and T. Tél, *Transient Chaos: Complex Dynamics on Finite Time Scales*, Applied Mathematical Sciences No. 173, 1st ed. (Springer Verlag, New York, 2011).
[43] E. G. Altmann, J. S. E. Portela, and T. Tél, Chaotic Systems with Absorption, Phys. Rev. Lett. **111**, 144101 (2013).
[44] A. E. Motter, M. Gruiz, G. Károlyi, and T. Tél, Doubly Transient Chaos, Phys. Rev. Lett. **111**, 194101 (2013).
[45] G. Casati, B. Chirikov, F. Izrailev, and J. Ford, in *Stochastic Behavior in Cassical and Quantum Hamiltonian Systems*,

Lecture Notes in Physics, Vol. 93, edited by G. Casati and J. Ford (Springer, Berlin, 1979), pp. 334–352.

[46] A. Bäcker, R. Schubert, and P. Stifter, Rate of quantum ergodicity in Euclidean billiards, Phys. Rev. E **57**, 5425 (1998); **58**, 5192(E) (1998).

[47] M. Degli Esposti and S. Graffi, in *The Mathematical Aspects of Quantum Maps*, Lecture Notes in Physics, Vol. 618, edited by M. Degli Esposti and S. Graffi (Springer-Verlag, Berlin, 2003), pp. 49–90.

[48] See Supplemental Material at http://link.aps.org/supplemental/10.1103/PhysRevLett.115.254101 for the derivation of Eq. (4) and the numerical computation of μ_γ for generic systems.

[49] J. Weber, F. Haake, P. A. Braun, C. Manderfeld, and P. Šeba, Resonances of the Frobenius-Perron operator for a Hamiltonian map with a mixed phase space, J. Phys. A **34**, 7195 (2001).

[50] K. Życzkowski and H.-J. Sommers, Truncations of random unitary matrices, J. Phys. A **33**, 2045 (2000).

[51] T. Micklitz and A. Altland, Semiclassical theory of chaotic quantum resonances, Phys. Rev. E **87**, 032918 (2013).

[52] J. Wiersig, Chiral and nonorthogonal eigenstate pairs in open quantum systems with weak backscattering between counterpropagating traveling waves, Phys. Rev. A **89**, 012119 (2014).

[53] C. T. West, T. Kottos, and T. Prosen, $\mathcal{PT}$-Symmetric Wave Chaos, Phys. Rev. Lett. **104**, 054102 (2010).

[54] H. Schomerus, From scattering theory to complex wave dynamics in non-Hermitian $\mathcal{PT}$-symmetric resonators, Phil. Trans. R. Soc. A **371**, 20120194 (2013).